THERMAL PERFORMANCE OF AN ELLIPTICAL PIN FIN HEAT SINK

Christopher L. Chapman, and **Seri Lee**
Aavid Engineering, Inc.
Laconia, New Hampshire 03247

Bill L. Schmidt
Silicon Graphics Computer Systems
Mountainview, California 94039

Abstract

Comparative thermal tests have been carried out using aluminum heat sinks made with extruded fin, cross-cut rectangular pins, and elliptical shaped pins in low air flow environments. The elliptical pin heat sink was designed to minimize the pressure loss across the heat sink by reducing the vortex effects and to enhance the thermal performance by maintaining large exposed surface area available for heat transfer. The performance of the elliptical pin heat sink was compared with those of extruded straight and cross-cut fin heat sinks, all designed for an ASIC chip. The results of the straight fin were also compared with those obtained by using Sauna™, a commercially available heat sink modeling program developed based on empirical expressions. In addition to the thermal measurements, the effect of air flow bypass characteristics in open duct configuration was investigated. As expected, the straight fin experienced the lowest amount of flow bypass over the heat sink. For this particular application, where the heat source is localized at the center of the heat sink base plate, the overall thermal resistance of the straight fin was lower than the other two designs mainly due to the combined effect of enhanced lateral conduction along the fins and the lower flow bypass characteristics.

Nomenclature

A_C	channel cross sectional area, m^2
A_f	fin surface area, m^2
A_p	projected area of heat sink base plate, m^2
A_{rad}	*effective* radiative surface area, m^2
A_w	wetted surface area, m^2
c_p	specific heat of air, kJ/kgK
D_h	hydraulic diameter, m
f	fanning friction factor
H	fin height, m
h	effective heat transfer coefficient, W/m^2K
h_m	bulk flow heat transfer coefficient, W/m^2K
j	Colburn factor
K	total dynamic resist ante coefficient
k_f	thermal conductivity of fin material, W/mK
L	characteristic length, m
m	fin parameter defined in Eq. (6), m^{-1}
$\dot{m}$	ma9s flow rate, kg/8
N_f	number of fins
Nu	Nusselt number
Pr	Prandtl number
Q	rate of total heat transfer, W
Q_{conv}	rate of convective heat transfer, W
Q_{rad}	rate of radiative heat transfer, W
R	overall thermal resistance, °C/W
R_{base}	conductive resistance of base, °C/ W
R_f	fin thermal resistance, °C/W
R_p	convective resistance of base, °C/ W
Re	Reynolds number
t	fin thickness, m
T_{amb}	ambient temperature, K
T_{in}	inlet air temperature, K
T_m	bulk mean air temperature, K
T_w	wall temperature, K
u_m	bulk mean flow velocity, m/s

Greek Symbols

ΔP	pressure drop, Pa
δ	thickness of base plate, m
ϵ	radiative surface ernissivity
η_f	fin efficiency
ρ	fiuid density, kg/m^3
σ	Stefan-Boltzmann constant, $5.67 \times 10^{-8} W/m^2K^4$

Introduction

As the amount of heat that needs to be removed from microelectronic devices constantly increases, thermal engineers are faced with never-ending challenges not only to provide innovative thermal designs but also to push the limits of the available technology and existing hardware. The heat sink industry, traditionally suppliers of cooling products, is always searching for new technologies which enhance thermal performance with no cost penalties. Heat sink features that incorporate findings from thermal re-

search and manufacturing breakthroughs are sought after as new product offerings. With this in mind, an elliptical shaped pin fin heat sink is of interest and needs to be investigated to find applicability as a general cooling product.

The thermal network of a finned heat sink consists of conductive, radiative, and convective resistances. From the junction of the device, heat is transported by conduction from the device through the interface and into the heat sink from which heat is usually removed by means of convection and radiation cooling. Fin efficiency and convection effectiveness can be examined to minimize any significant conduction resistance though the fins and improve the overall performance of the heat sink. There exists significant work carried out in the thermal analysis of heat sink design. An analytical approach was taken by Keyes [1] who developed formulas for the fin and channel dimensions that provide optimum cooling under various forced convection cooling conditions. Bartilson [2] investigated, using both experimental and numerical techniques, air jet impingement cooling on a rectangular pin-fin heat sink. Various shapes of longitudinal straight fin heat sinks were experimentally examined, and the thermal performance measurements were compared with existing correlations [3]. Kishimoto and Sasaki [4] examined cooling characteristics of a staggered, diamond-shaped pin fin heat sink, and Lee et. al [5], and Sparrow and Kadle [6] investigated the effect of air flow bypass through tip-to-shroud clearance.

A study of heat sink fin technologies has given information toward important design criteria for practical cooling of electronic components. An elliptical pin fin heat sink was developed with specific design parameters; maintaining large exposed surface area for heat transfer and minimizing vortex flow by incorporating an air foil design. The air foil design in the shape of an ellipse was chosen to reduce boundary layer buildup and any vortex affect. The result in a microelectronic environment is minimized downstream air heating and less pressure drop especially when multiple heat sinks are placed in series. The application includes ASIC chips arranged behind each other in the direction of the air flow. This specific multiple heat sink design feature is not investigated here. Rather, the thermal performance of a single elliptical pin fin heat sink was examined, and the results are compared with those of other type of heat sinks as a qualification study for general usage. For comparison, equal volume heat sinks were prepared using cost effective, existing heat sink technologies. In Figure 1, they are represented as straight and cross-cut heat sinks. The elliptical pin heat sink is made of cast aluminum, and the cross-cut and straight fin heat sinks are made of extruded aluminum. The present study is a generalized comparison in which the effects that the differences in thermal conductivity, flow characteristics, and pressure drop have on the heat sink performance are measured in terms of the thermal resistance (from the heat sink surface to the ambient air) and the amount of flow bypass.

Thermal Modeling

The design of elliptical pin heat sinks challenges existing thermal modeling techniques. It is generally accepted that the most comprehensive modeling for a heat sink system would be computational fluid dynamics (CFD). Either by using a finite volume or finite difference method, the actual phenomena at the fin surface can be quantified. Unfortunately, significant modeling and run time is needed to accurately represent small pins with complex meshing. A second technology, finite element analysis (FEA) can also be useful in determining performance, especially conductivity gradients. The heat transfer coefficient can be determined using advanced FEA codes which incorporate fluid mechanics. However, pin fin geometry cannot easily be modeled by using either method. Each pin must be individually discretized, increasing the modeling time substantially. The approach taken in this paper was to compare this elliptical shaped heat sink with a conventional extruded fin heat sink of equal volume. Comparative testing can be correlated with accepted rectangular fin modeling techniques. The use of empirical correlations and analytical modeling has been traditionally focused at rectangular longitudinal fins. As a control, this straight fin heat sink can be tested against a cross-cut equivalent and the elliptical pin heat sink.

A simulation program has been developed for predicting and optimizing thermal performance of hi-directional

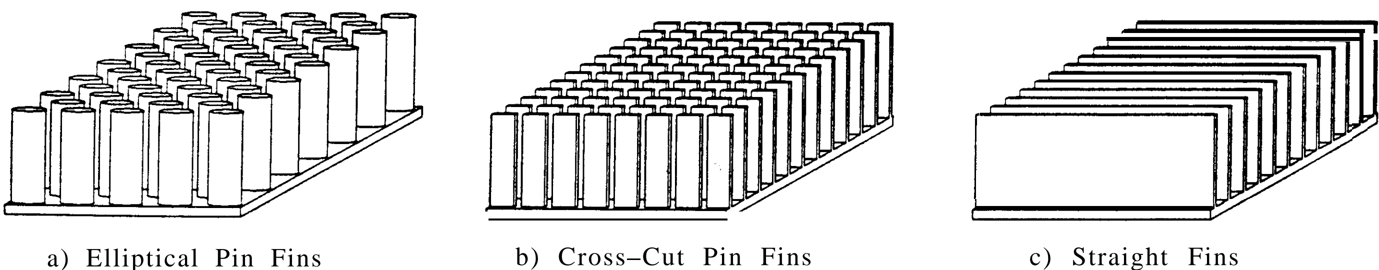

Figure 1: Schematic diagram of heat sinks.

fin heat sinks placed in a rectangular wind tunnel. The program utilizes the basic heat transfer and fluid-friction performance data presented in graphical forms in reference [7], where the fanning friction factor, f, and the dimensionless heat transfer coefficient, Colburn j factor, are provided as functions of the Reynolds number for rectangular tubes of various aspect ratios. By curve-fitting and interpolating the provided plots, one can determine the pressure drop and the average heat transfer coefficient for a fluid flow inside a rectangular tube. The computed values can then be subsequently used as approximations for the open rectangular channels formed between adjacent fins of a straight heat sink as follows.

Upon obtaining the f and j factors from the plots [7] for a given channel and the flow velocity, the total pressure drop, AP, and the average heat transfer coefficient, h_m, can be computed from

$$\Delta P = \left(f\frac{A_w}{A_c} + K\right)\frac{\rho u_m^2}{2} \quad (1)$$

$$h_m = j\ Re\ Pr^{1/3}\frac{k}{D_h} \quad (2)$$

where A_w and AC are the wetted surface area and the cross sect ional area of the channel, respectively, and K is the total dynamic resistance coefficient accounting for the pressure losses due to entrance and exit effects. The K values can be estimated from the plots provided in [7] or [8]. Re is the Reynolds number based on the bulk mean channel flow velocity u_m and the hydraulic diameter D_h. Pr is the Prandtl number, and k is the thermal conductivity of the fluid.

However, the above heat transfer coefficient is defined based on the temperature difference between the channel wall and the bulk flow:

$$h_m = \frac{Q_{conv}/A_w}{T_w - T_m} \quad (3)$$

Therefore, in order to determine the effective heat transfer coefficient based on the temperature difference between the channel wall and the inlet flow $(T_w - Tin)$, one needs to use the following expression, which is developed by balancing the total heat transfer into the fluid with the enthalpy increase in the flow from the inlet to the outlet of the channel:

$$h = \frac{\dot{m}c_p\{1 - exp[(h_m A_w)/(\dot{m}c_p)]\}}{A_w} \quad (4)$$

where m is the mass flow rate, and c_p is the specific heat.

The modeling also incorporates the accepted correlations for the Nusselt number from [9]. In forced convection from parallel plates, it must be determined whether the plates are isolated, and if the flow is turbulent. The criteria, adopted for isolation, is that the air gap between plates is five times the thickness of the isolated plate boundary layer [10]. The critical Reynolds number for determining turbulence is 2,200. This is a low value since there are significant entrance effects and high free stream turbulence associated with an array of parallel plates.

The turbulent flow models used are represented by the following equations [9]:

$$Nu = 0.023\ Re^{0.8}Pr^{0.3}(1 + 1.68\ (D_h/L)^{0.58}) \quad \text{for } 2 < L/D_h \leq 20 \quad (5)$$

$$Nu = 0.023\ Re^{0.8}Pr^{0.3}(1 + 6\ (D_h/L)) \quad \text{for } L/D_h > 20 \quad (6)$$

Upon obtaining the effective heat transfer coefficient from the above equations, the fin efficiency η_f can be computed, assuming negligible heat dissipation through the edge surfaces [11], as

$$\eta_f = \frac{\tanh\ mH}{mH} \quad (7)$$

with

$$m = \sqrt{\frac{2h}{k_f t}} \quad (8)$$

where H and t are the fin height and the fin thickness, and k_f is the thermal conductivity of the fin material. The fin thermal resistance then becomes

$$R_f = \frac{\eta_f}{hA_f} \quad (9)$$

where A_f is the fin surface area, and the overall heat sink thermal resistance R can be easily computed from the following thermal network expression:

$$R = \left[\frac{N_f}{R_f} + \frac{1}{R_p}\right]^{-1} + R_{base} \quad (10)$$

with

$$R_p = \frac{1}{hA_p} \quad (11)$$

$$R_{base} = \frac{\delta}{k_f A_p} \quad (12)$$

where N_f is the number of fins, A_p the projected area of the heat sink base plate and δ the thickness of the base plate.

The model equation, used for radiation heat loss in parallel mode with convection heat transfer (see Figure 2), is the Stefan-Boltzmann equation:

$$Q_{rad} = \epsilon\sigma A_{rad}(T_w^4 - T_{amb}^4) \quad (13)$$

where T_w and T_{amb} are the absolute surface and ambient temperatures, respectively.

A commercial package is available which incorporates the above expressions. Sauna'M from Thermal Solutions, Inc. [10] is a conjugate thermal modeling tool which incorporates computer aided design and heat transfer. The modeling and run times are only a fraction of those required with CFD and FEA analyses. This software allows for accurate modeling of the heat sink base plate with fins by accounting for conduction heat transfer in the base plate as well as convection and radiation heat transfer from the exposed surfaces. The thermal gradients are predicted along the entire heat sink base plate. The local temperatures are obtained at the locations where thermocouples are placed in the test samples.

Measurement

The test samples included elliptical pin finned, extruded straight finned, and extruded cross-cut finned (rectangular pin fins) heat sinks. The elliptical pin heat sink was made of cast aluminum alloy. Although, the thermal conductivity is two-thirds that of an extrusion alloy, the specific pin detail can only be made economically by this process. Each pin is in the shape of an ellipse with a major axis of 5.54 *mm* and a minor axis of 1.27 *mm.* However, the leading and trailing ends of the ellipse came to a sharp edge, simulating the airfoil feature. The 105 pins were staggered with an outer grid being 10 x 6 and an inner grid of 9 *x* 5. In order to determine the applicability of this shape in heat sink design, similar test samples with conventional rectangular longitudinal extruded fins were made.

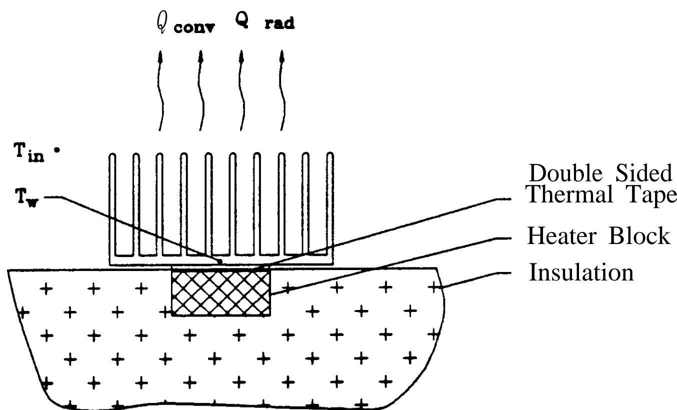

Figure 2: Thermal test module.

The heat sink extrusion chosen for this testing has ten 1.52 *mm* thick fins equally spaced across 58.42 *mm.* The overall height of the profile was 29.21 *mm* with a base thickness of 2.54 *mm.* Two extruded heat sinks were made and one had an additional manufacturing process called cross-cutting. This material removal enables air to pass through pins in a manner similar to the elliptical pin fin design, There were nine cuts along the 58.42 *mm* length, and each cut removed 1.52 *mm* of material with 4.32 *mm* long pins. All three heat sinks have equal volume, and the total surface area was also calculated to be nearly identical. Since the cross-cutting operation removed material in width which was the same size as the fin thickness, no difference in surface area is seen between the straight and cross-cut heat sinks. Using the complete elliptic integral of the second kind to determine the perimeter of each ellipse, the total exposed surface area of the elliptical pin heat sink was calculated to be 339.2 cm^2 compared to 346.8 cm^2 for the extruded heat sinks.

Each heat sink had a finish with an estimated emissivity of 0.8 minimum. This was done by black sulfuric acid anodizing the extruded heat sinks, and using black paint for the cast elliptical pin heat sink. Thus, radiative heat transfer was included in the testing and combined with the convection component to represent parallel heat transfer from the surface of the fins, as depicted in Figure 2.

A central backside pedestal 25.4 *mm* square was machined into the extruded samples and cast into the elliptical pin fin heat sink. This simulated an actual design feature in order to properly contact the semiconductor die. The surface was covered with a double sided thermal tape which held the heat sink to a heater block simulating the device. A pneumatic piston fixture was used to apply 1.93 MPa of mounting pressure for five minutes at the interface. The conductive thermal resistance from the copper block to the heat sink surface was designed to be constant and is not included in the thermal resistance values obtained. The block was insulated using Styrofoam, so that only the heat sink was exposed to the air flow. The shape of this copper block was designed to replicate the ASIC chip for which the elliptical heat sink was designed for. Two Caddock Kool Tab TO-220 resistors were soldered to the copper block as heat sources. Each 20Ω resistor was measured to be within 1% of the rating. A Lambda LQ-532 power supply was used to provide up to 20 watts into each resistor, resulting in the total heat flux of 40 W/in^2, or 6.2 W/cm^2. The power was determined using a Micronata Multimeter 22-186A to measure the voltage drop across each resistor.

The temperature measurements were taken using Omega T-36SLE copper constantin thermocouples 0.43 *mm* in diameter. Three temperatures were taken throughout the experiment, the ambient air 150 *mm* upstream of the heat sink, the heat sink pedestal, and the copper block. The heat sink and ambient temperature difference waa used to represent heat sink performance. Both the heat sink and block thermocouples were inserted into a 1.0 *mm* di-"

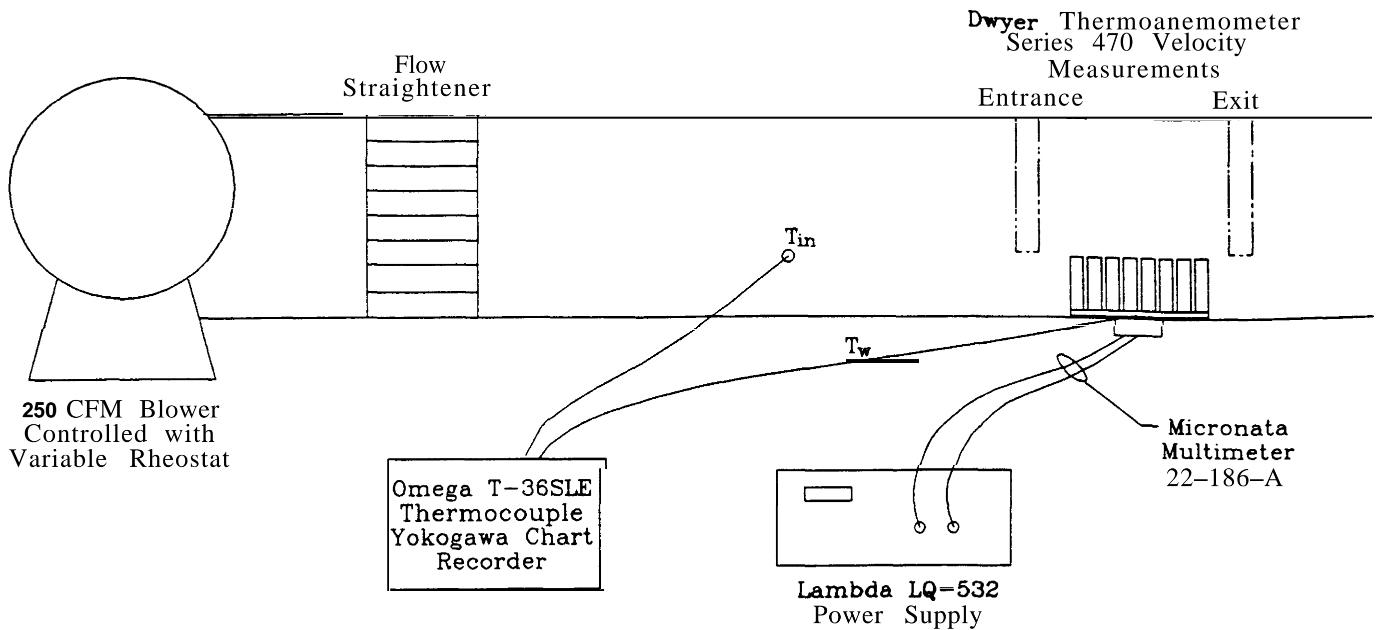

Figure 3: Experimental test set-up.

ameter hole which was drilled 3.18 *mm* deep and filled with thermal grease and thin copper wire. The thermal grease used was silicon based with a thermal conductivity **of 0.004** *W/mK.* The thermocouples were calibrated to within O. 1°C of each other. **A** Yokogawa chart logger was used to record the temperatures throughout the experiment, including the startup transient response and steady-state equilibrium.

The actual testing was done in compliance with the recommended test procedures outlined by the Electronics Industries Association's Components Bulletin #5. The purpose of this standard is to establish procedures for the evaluation, calibration, and presentation of test data for serniconductor heat sinks. It covers temperature measurement, thermocouple mounting, ambient conditions, and test data presentations.

The test set-up is shown in Figure 3. All testing was performed in a plexiglas wind tunnel measuring_ 254 *mm* by 127 *mm* by 1830 *mm* long. The 250 CFM (118 Liters/sec.) blower was controlled using a variable rheostat. The volumetric air flow was not monitored since the local air veloc-it y was measured. Flow straighteners were used to evenly distribute the flow direction, minimizing turbulence. The air velocity was recorded using a Dwyer Series 470 thermoanemometer. The duct velocity was measured 300 *mm* upstream of the test piece. A second measurement was taken as an average velocity through each fin at the exit of the heat sink. The amount of flow bypass is the difference of these values. All velocity measurements were made after steady state was established. The testing environment simulates an actual heat sink application in which flow can either be left in an open duct where air flow can bypass the fin array or directed through the heat sink by placing a flow blockage around the heat sink. In Figure 4, these configurations were termed open and confined flow respectively. The confined test setup had a 3.8 *mm* **gap** around **the heat sink allowed for air flow.**

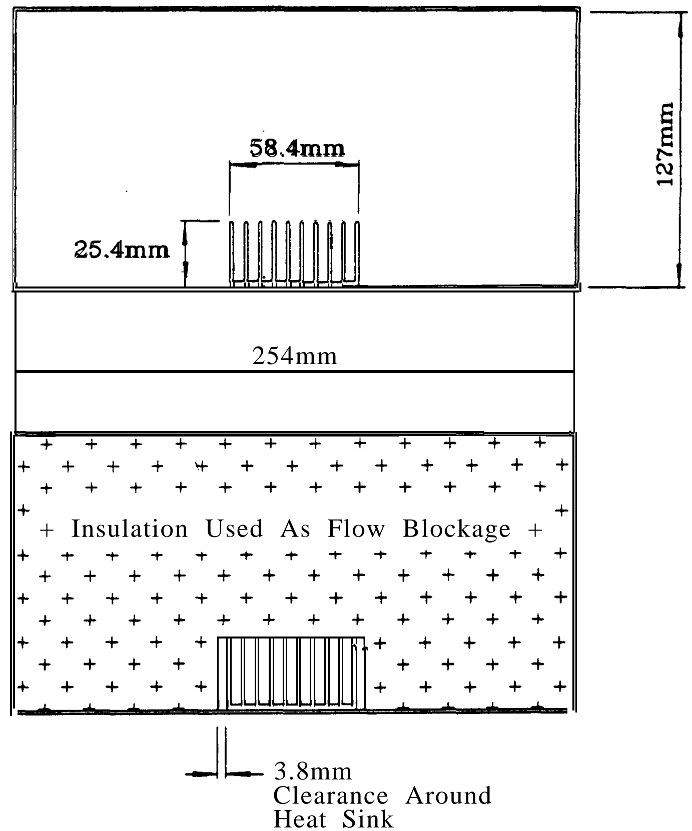

Figure 4: Open and confined flow configurations.

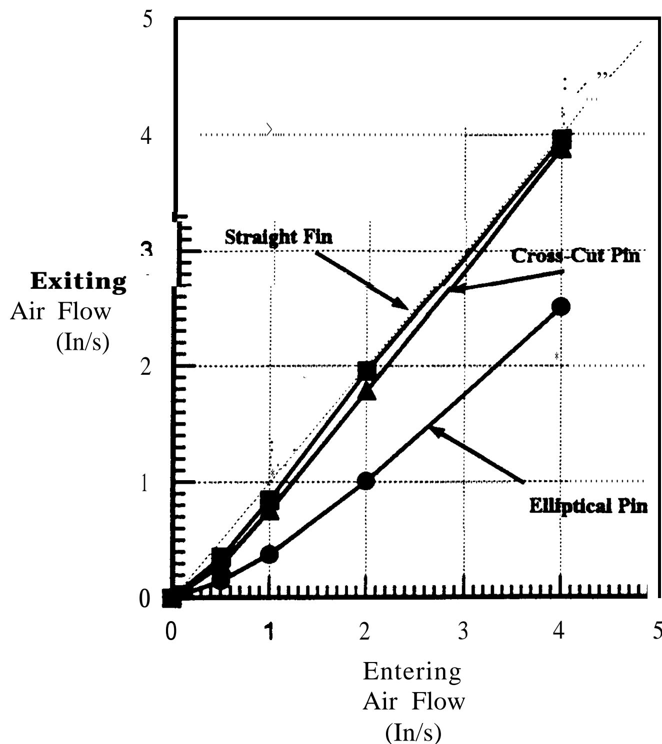

Figure 5: Dynamic correlation of effective air flow through a heat sink placed in an open flow configuration.

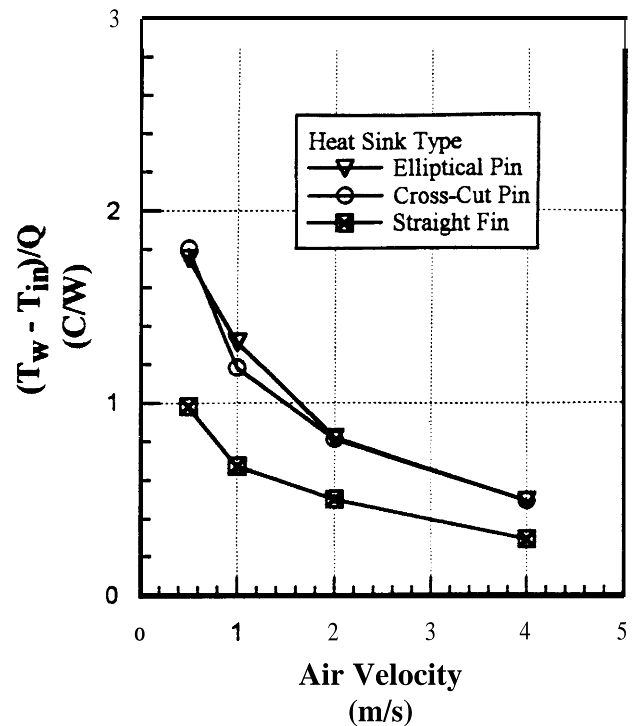

Figure 6: The comparative thermal resistance for open air flow testing.

Results and Discussions

The effect of testing in an open flow is shown in Figure 5, where significant flow bypass is seen with the elliptical heat sink. This is of no surprise since the cross-section of this heat sink represents more of an obstruction for airflow. Also, the cross-cuts induced more flow bypass than the straight fin, suggesting increased turbulence and pressure drop. For ail heat sinks, the largest amount of bypass is at an air velocity between 0.5 and 1.0 *m/s.* This low-flow phenomenon has been reported and leads to a design optimization analysis that is similar to the analysis used in determining the natural convection optimum fin spacing.

The overall thermal performance of each heat sink in open flow is shown in Figure 6 where the thermal resistance, defined as $(T_w - T_{in})/Q$, is the power independent temperature relation of heat sink performance. Due to minimal flow bypass already seen with the straight fin, it is of no surprise that this heat sink was cooler. Also seen is equal thermal performance between the elliptical pin and cross-cut fin heat sinks, As can be seen from Figure 5, the exiting air flow through the elliptical pin heat sink was 60% of that with the cross-cut heat sink. This suggests that the elliptical airfoil shape has an improved heat transfer coefficient which is not directly related to the air flow velocity. This phenomena has been quantified in the elliptical pin fin development but had not yet been published.

Figure 7 shows the thermal performance in confined air

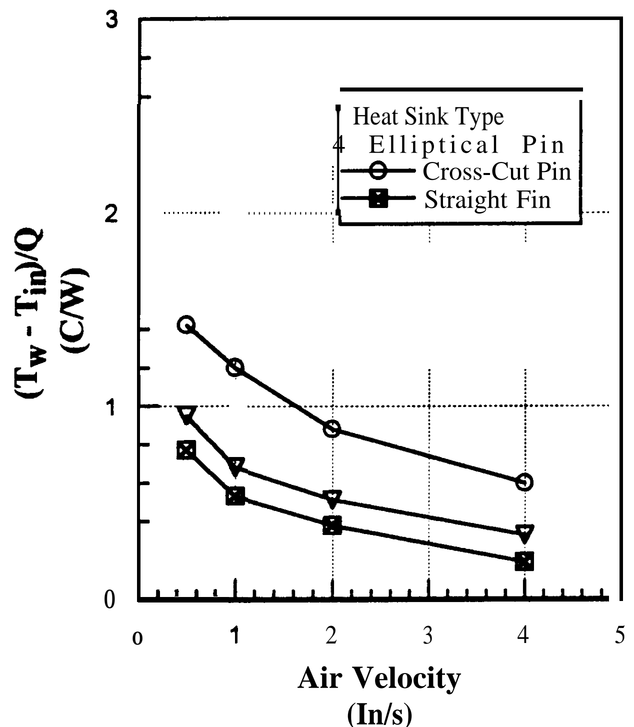

Figure 7: The comparative thermal resistance for confined air flow testing.

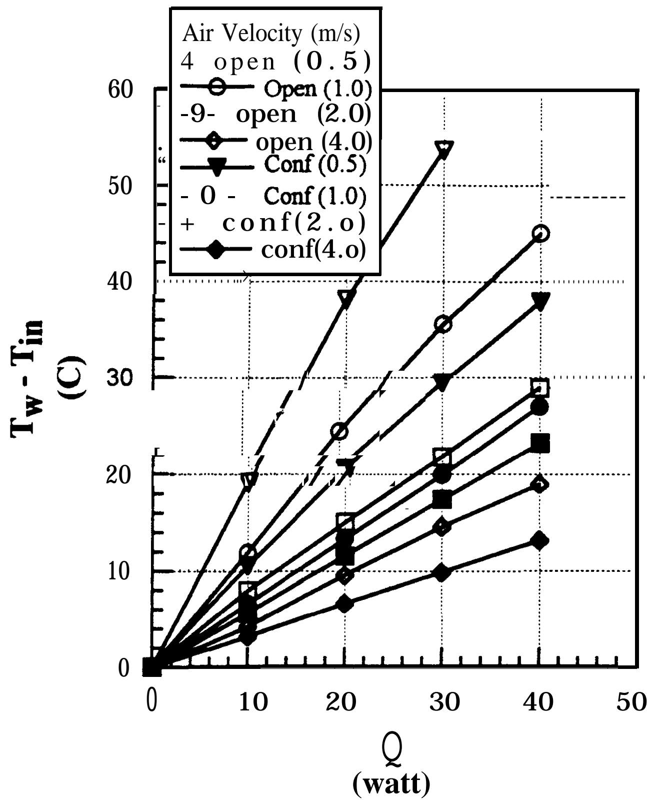

Figure 8: Forced convection performance of elliptical pin fin heat sink based upon entering air velocity into the test chamber for both open and confined flow configurations.

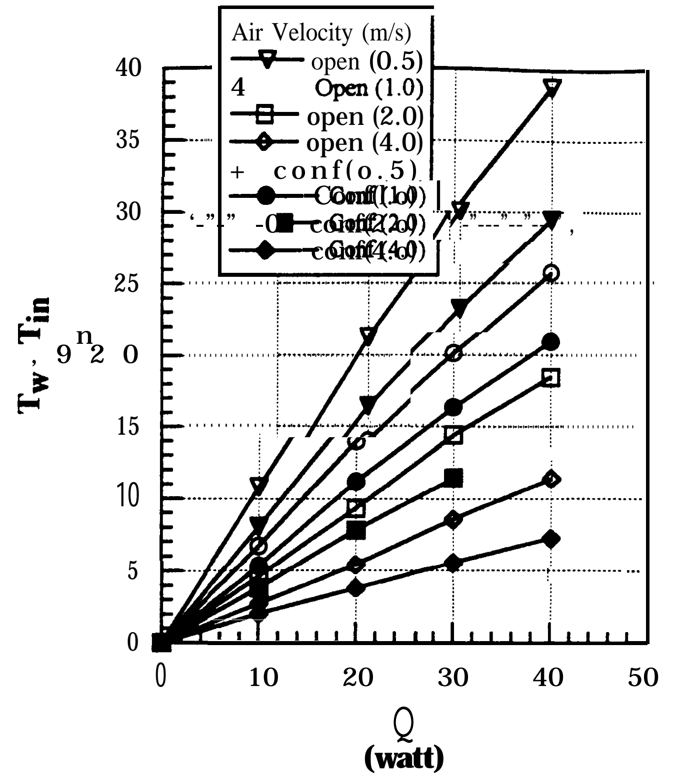

Figure 9: Forced convection performance of straight fin heat sink based upon entering air velocity into the test chamber for both open and confined flow configurations.

flow where the velocity through each heat sink is the same. Once again, the straight fin performed best. This was an unexpected result, but can be explained by looking at the overall heat sink efficiency. Much emphasis in heat sink design is spent looking at fin efficiency. However, with increasing heat flux in microelectronic applications, the efficiency of how fins conduct laterally may have been overlooked. The straight fin allows for an improved lengthwise conduction path other than just through the base. Both pinned versions have an overall higher conduction resistance, since the pins directly over the 25.4 *mm* square heat source are at a higher temperature than the surrounding outer pins, Further testing including infrared spectroscopy can quantify this effect.

The measured temperature rises, plotted in Figure 8 for the open and confined flows over the elliptical pin heat sink, reveal the thermal effect of bypass air in the open configuration. Other elliptical pin configurations with a more open cross sectional area may result in less flow bypass. In Figure 9, the result of the straight fin heat sink shows less of an effect of the open configuration as expected, since the exiting flow velocity is nearly identical to the entrance velocity.

The thermal modeling using Sauna™ was performed on the straight fin heat sink. Figure 10 is a comparison between the experimental data and the modeling. For low air

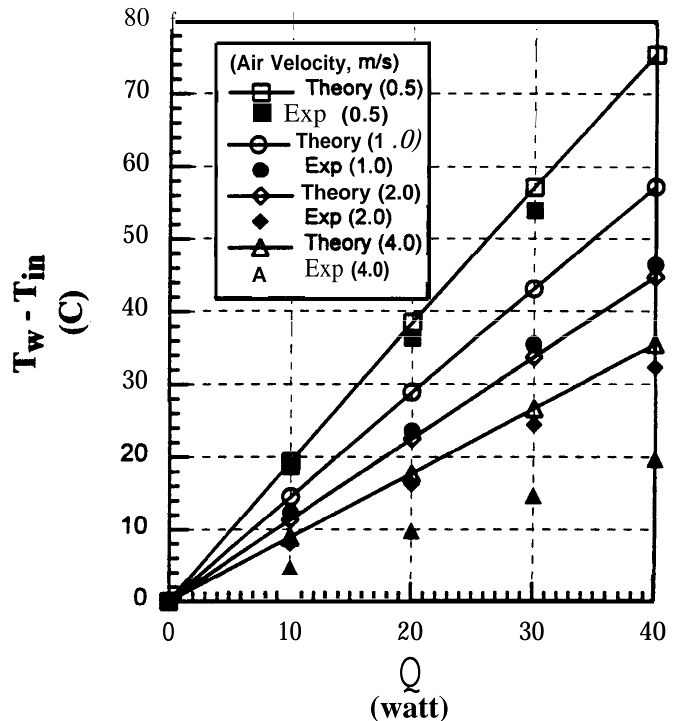

Figure 10: Comparison of theoretical predictions with experimental measurements for the extruded straight fin heat sink.

velocity, the predictions are in good agreement. However, poor agreement is observed for higher flow velocities, suggesting that the turbulence effects in the wind tunnel may not be accurately modeled in the analysis. This may result from the low critical Reynolds value used in Sauna™ for turbulent flows.

Conclusions

The testing described in this paper incorporates several possible performance factors into two terms; flow bypass and overall thermal resistance. These simplified terms represent a combination of several factors, such as material conductivity, lateral fin conduction, boundary layer formation, effective surface area, and pressure drop. In comparing the elliptical pin heat sink with the rectangular pin heat sink, the air foil benefits are visible. There was 40% more air flowing through the rectangular pin design, yet the thermal resistances were virtually equal. The elliptical pin enhances heat transfer. These results are in correlation with the basis of the elliptical pin fin design considerations; i.e. reduced vortex flow, eliminating boundary layer effects. Another surprising result was that the extruded straight design performed significantly better than either of the other two designs over the flow range examined herein.

The comparison between the extruded and rectangular pins at similar air bypass indicates a performance factor not considered previously. The effect of lateral fin conduction is significant at either high air velocities (> 3 m/s) or at high heat flux. The heat flux of 6.2 W/cm^2 is rather significant for this size of heat sink and low air flows. A design principle of heat sinks which is often assumed is the ability to cool in an omni-directional air flow environment. The cross-cut heat sink offers ease of production assembly where misalignment of the heat sink with respect to the direction of air flow will not result in a failure.

Further study is needed to quantify two key design parameters. The effect of heat flux and air flow relating to lateral fin conduction. This study would allow the increasing power devices currently being developed to use cost effective air cooled heat sinks. This lateral conductance may lead to reducing the need for additional spreader plates and possible heat pipes. If the fin is used as the transport means of heat, more effective and less costly designs will be apparent.

The elliptical pin heat sink test ed represents only one set of design parameters relating pin spacing and shape based upon minor and major axes. There may exist other designs which produce better results in overall thermal performance. A study looking at reduced spacing, pin alignment, pin staggering, and an array of ellipse axis ratios would be advantageous to the heat sink industry.

Acknowledgments

The authors would like to thank Mr. Raul Rodriguez for his assistance in experimental apparatus setup, Mr. Joshua West for running the test and recording data, and Mr. Ron Lavochkin for his valuable comments during the preparation of this manuscript. Thanks also go to Mr. Rick Gagnon for his assistance in preparing the figures.

References

1. R.W. Keyes, "Heat Transfer in Forced Convection Through Fins," *IEEE Transactions on Electronic Devices,* Vol. ED-31, No, 9, pp. 1218-1221, 1984.

2. B. W. Bartilson, "Air Jet Impingement on a Miniature Pin-Fin Heat Sink," ASME Paper No. 91-WA-EEP-41, 1991.

3. H. Matsushita and T. Yanagida, "Heat Transfer From LSI Packages With Longitudinal Fins In a Free Air Stream," *Advances in Electronic Packaging,* ASME Proceedings, EEP-VO1. 4-2, pp. 793-800, 1993.

4. T. Kishimoto and S. Sasaki, "Cooling Characteristics of Diamond-Shaped Interrupted Cooling Fin For High-Power LSI Devices," Electronics Letters, Vol. 23, pp. 456-457, 1987.

5. R.S. Lee, H.C. Huang and W.Y. Chen, "A Thermal Characteristic Study of Extruded Type Heat Sinks In Considering Air Flow Bypass Phenomenon," Proceedings of the 6th Annual IEEE Semiconductor Thermal and Temperature Measurement Symposium, pp. 95-102, 1990.

6. E.M. Sparrow and D.S, Kadle, "Effect of Tip-to-Shroud Clearance on Turbulent Heat Transfer From a Shrouded, Longitudinal Fin Array," *ASME Journal of Heat Transfer,* Vol. 108, pp. 519-524, 1986.

7. W.M. Kays and A.L. London, *Compact Heat Exchangers,* 3rd Ed., McGraw-Hill Company, New York, 1984.

8. I.E. Idelchik, *Handbook of Hydraulic Resistance,* 2nd Ed., Hemisphere Publishing, New York, 1986.

9. G. Ellison, *Thermal Computations For Electronic Equipment,* Van Nostrand Reinhold Co., New York, 1984.

10. M. Naughton, *Sauna 'M User Manual,* Version 2.10-2, Thermal Solutions, Inc., 1992.

11. F.P. Incropera and D.P. DeWitt, *Fundamentals of Heat and Mass Transfer,* 3rd Ed., John Wiley & Sons, New York, N.Y,, 1990.